Geoscience Frontiers 7 (2016) 821–834

HOSTED BY

Contents lists available at ScienceDirect

China University of Geosciences (Beijing)

Geoscience Frontiers

journal homepage: www.elsevier.com/locate/gsf

Research paper

Depositional environments and sequence stratigraphy of the Bahram Formation (middle–late Devonian) in north of Kerman, south-central Iran

Afshin Hashmie*, Ali Rostamnejad, Fariba Nikbakht, Mansour Ghorbanie, Peyman Rezaie, Hossien Gholamalian

Department of Geology, Faculty of Sciences, University of Hormozgan, Bandarabbas, Iran

ARTICLE INFO

Article history:
Received 7 October 2014
Received in revised form
24 June 2015
Accepted 8 July 2015
Available online 6 August 2015

Keywords:
Bahram Formation
Devonian
Facies analysis
Mixed carbonate-detrital shallow-shelf
Sequence stratigraphy
Tabas block

ABSTRACT

This study is focused on sedimentary environments, facies distribution, and sequence stratigraphy. The facies and sequence stratigraphic analyses of the Bahram Formation (middle–late Devonian) in south-central Iran are based on two measured stratigraphic sections in the southern Tabas block. The Bahram Formation overlies red sandstones Padeha Formation in sections Hutk and Sardar and is overlain by Carboniferous carbonate deposits of Hutk Formation paraconformably, with a thickness of 354 and 386 m respectively. Mixed siliciclastic and carbonate sediments are present in this succession. The field observations and laboratory studies were used to identify 14 micro/petrofacies, which can be grouped into 5 depositional environments: shore, tidal flat, lagoon, shoal and shallow open marine. A mixed carbonate-detrital shallow shelf is suggested for the depositional environment of the Bahram Formation which deepens to the east (Sardar section) and thins in southern locations (Hutk section). Three 3rd-order cyclic siliciclastic and carbonate sequences in the Bahram Formation and one sequence shared with the overlying joint with Hutk Formation are identified, on the basis of shallowing upward patterns in the micro/pertofacies.

1. Introduction

During the Silurian and Devonian, parts of Iran (central Iran, Alborz and Sanandaj-Sirjan) along with the Afghan and Turkish plates were attached to the Arabian and African plates and formed the northwestern margin of Gondwana and the southern margin of the Paleo-Tethys (Berberian and King, 1981; Husseini, 1991; Sharland et al., 2001; Ruban et al., 2007; Al-Juboury and Al-Hadidy, 2009). Devonian rocks are widely distributed and superbly exposed in the south-Tabas block of central Iran (Fig. 1). Throughout the Devonian period Iran was situated consistently within the southern hemisphere at a latitude close to 30° (Scotese and McKerrow, 1990, see Fig. 1). The Devonian rock units are the Juban Formation in Saudi Arabia, Kuwait (partly), Chalki volcanics, Pirispiki, Kaista and part of Ora formations in Iraq, the Yeginili Pendik and Buykecell formations in Turkey, Khoshyilagh Formation in Alborz Iran and parts of Muli and Zakeen formations in NW and South of Iran (Zagros) respectively (Husseini, 1991; Ghavidel-Syooki, 1994; Al-Sharhan and Narin, 1997; Al-Hajri and Filatoff, 1999; Brew and Barazangi, 2001; Sharland et al., 2001; Wendt et al., 2002, 2005; Laboun, 2010; Wehrmann et al., 2010; see Fig. 2) and the Bahram Formation in central Iran. Ruttner et al. (1968) named and measured the Bahram type section in the Ozbak-kuh Province about 150 km north of Tabas it is composed of grey to dark grey limestone with intercalation of grey shale and marl. Unfortunately, Ruttner et al. (1968) had chosen the Ozbak-Kuh Mountains as type localities for his newly established formation but few other areas in Iran appear less suitable for such a lithostratigraphic framework (Wendt et al., 2002). Due to the abundance of brachiopods, it was called “brachiopod skalk” that is interval overlying the Sibzar and underlying the Shishtu Formation (Flugel and Ruttner, 1962). Later by Stockline et al. (1965) they use the name Bahram Formation for the beds. Lithology of Bahram Formation is different in other areas of central Iran. On the other hand, the Bahram Formation in north of Kerman is mostly composed of carbonate and clastic rocks

* Corresponding author.
E-mail address: hashmieafshin@gmail.com (A. Hashmie).
Peer-review under responsibility of China University of Geosciences (Beijing).

http://dx.doi.org/10.1016/j.gsf.2015.07.002

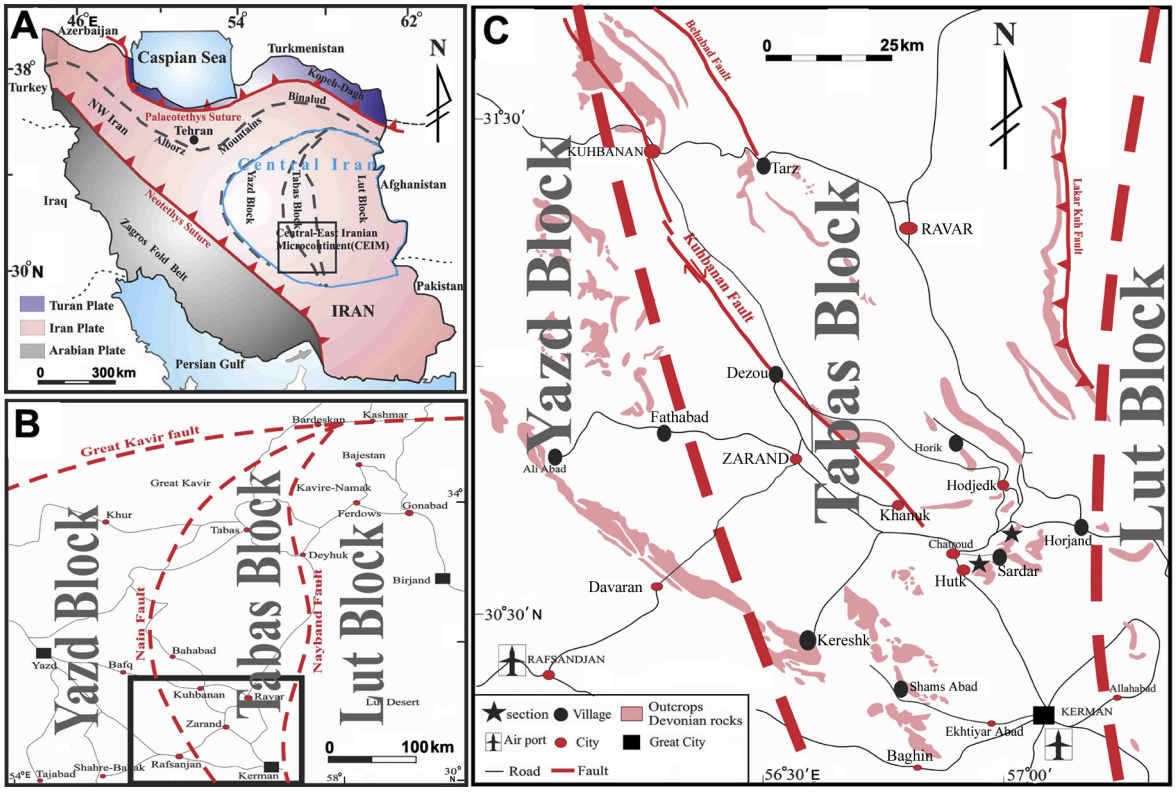

Figure 1. Location map of the study area and measured stratigraphic sections in south-central Iran. (A) Structural and geographic framework of Iran showing the main sutures, structural units and geographic areas; (B) close-up view of black square in (A), south-central Iran. Subdivisions of the central Iran province and location of the south Tabas block (modified from Wilmsen et al., 2010; Zand-Moghadam et al., 2014); (C) close-up view of black-square in (B), distribution of Devonian rocks in the Kerman–Kuhbanan–Ravar area and the locations of measured sections in south Tabas block (modified from Wendt et al., 2002).

(Huckriede et al., 1962; Vahdati-Daneshmand et al., 1995; Wendt et al., 2002). The regional geology and stratigraphy of the Kerman area have been described by Huckriede et al. (1962) and Wendt et al. (2002, 2005). The fossil content of the Bahram Formation has been illustrated by various authors and includes: brachiopods (Dastanpour and Bassett, 1998), trilobites (Morzadec et al., 2002), crinoids (Webster et al., 2003), acritarchs and miospheres (Ghavidel-syooki and Mahdavian, 2010) and conodonts (Gholamalian, 2003, 2007; Gholamalian and Kebriaei, 2008; Gholamalian et al., 2009; Bahrami et al., 2011). Few previous studies focused on the depositional environments of the Bahram Formation, especially in the Tabas block. The most comprehensive study on the Devonian rocks in Iran was carried out by Wendt et al. (1997, 2002, 2005). They believed that the middle–late Devonian rocks (Bahram Formation) were deposited mainly on a shallow carbonate platform at the northern margin of Gondwana that is delineated by land areas in the north (eastern Alborz), southeast (Yazd Block), and southwest (Zagros). The main scope of this study is to study the facies and sequence stratigraphy of middle–late Devonian (Bahram Formation) and to identify sedimentary environments in two different regions (Hutk section, 25 km along the Kerman-Zarand road, next to Hutk city; and Sardar section, 3.5 km east of Hossein-Abad and 49 km north of Kerman). Finally, based on facies variation, we analyzed the sequence stratigraphy of the Bahram Formation (sections) in south Tabas block in central Iran (Fig. 1).

2. Geological setting and study area

In Iran, Devonian successions are exposed in limited places. They are most complete and widespread in the eastern and central Alborz and central Iran (Wendt et al., 2005). The study area is located in the central part of the Central-East Iranian Microcontinent (CEIM; Takin, 1972; Stocklin, 1974; see Fig. 1A). The CEIM, together with central Iran and the Alborz Mountains, forms the Iran Plate, which occupies a structural key position in the middle eastern Tethysides (Sengor et al., 1988; Sengor, 1990). The CEIM consists of three north-south oriented structural units, called the Lut, Tabas, and Yazd blocks (Fig. 1), which are now aligned from east to west, respectively (Stocklin, 1968, 1977). The Tabas block is bounded by the Great Kavir Fault in the north, the Nain Fault in the west and the Nayband Fault in the east (Fig. 1C). Tectonically the area is part of a foreland basin filled dominantly with a thick sequence of clastic and carbonate sediments. The two mentioned regions show remarkable outcrops of the Bahram formations (Fig. 3), which is affected by the structural impressions (faults) and also petrological nature of the formations. Long strike faults (which have cut the anticlines longitudinally and opened them laterally by erosion), short faults (which cut them widthwise) and lineaments which are of structural and stratigraphical origins are typical structural elements in the regions, exhibiting a low morphology and more or less change in thicknesses. The older crustal blocks are relatively rigid, whereas the surrounding strata are more easily deformed into mountains and fault zones, a broken, mountainous belt separates the Tabas blocks. The Kouhbanan Fault (a branch of Nain Fault) zone defines the straight, sharp area margin of the Tabas block. Early to middle Cambrian volcanic rocks of the Rizu complex blanketed the oldest lithostratigraphic units in the studied area which compound early Cambrian red sandstones and shales of the Zaigun and Lalun formations (Fig. 3).

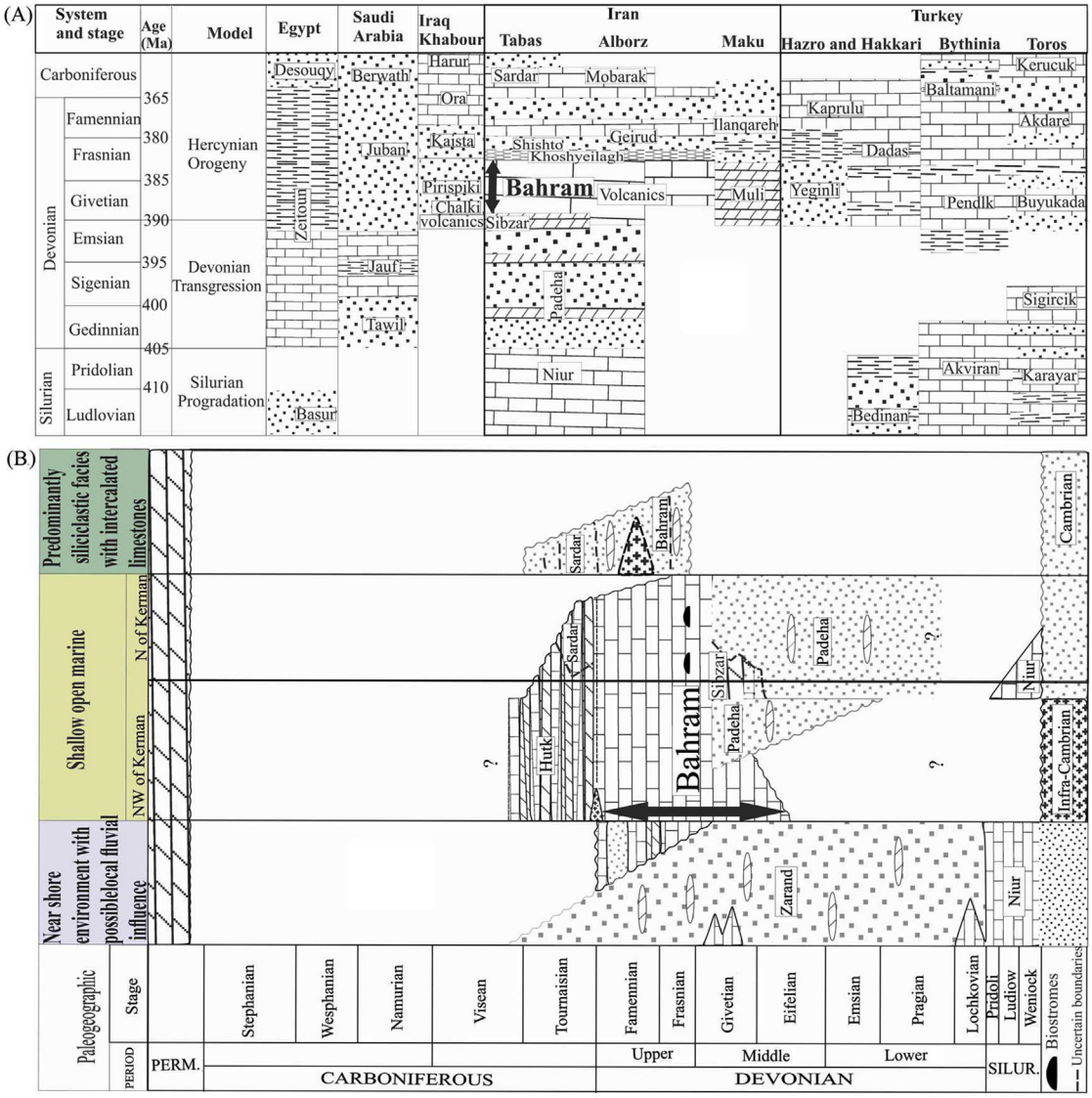

Figure 2. (A) Stratigraphic correlation chart of the Devonian rock units of Iran, Iraq, Saudi Arabia, Egypt and Turkey (with slightly modified after Husseini, 1991). (B) Stratigraphic correlation chart of the Silurian to Permian units in the Kerman–Kuhbanan–Ravar area (with slightly modified after Wendt et al., 2002). For legend see Fig. 4.

3. Methodology

Two stratigraphic sections of the middle to late Devonian succession were measured, sampled and described reflecting coeval environments along north direction (Kerman) (Fig. 1). The sections were described in the field, including their weathering profiles, size, color, lithology, relevant characteristics of the beds in vertical succession, lateral variations when there were changes in the sedimentation facies and bedding surfaces. 182 uncovered thin sections were produced (86 thin sections from the Hutk section and 96 thin sections from the Sardar section). Some samples of limestone have been analyzed to ensure about phosphorite contents. All thin sections were checked under the microscope for petro/microfacies analysis. The terminology of limestones and dolostones is based on the classification introduced by Dunham (1962) and Embry and Klovan (1971). The petrographic description of the sandstones follows Pettijohn et al. (1987). The mud rocks classification follows the scheme of Dorrik (2010). Facies definition was based on the microfacies characteristics, including depositional texture, grain size, grain composition, energy index classification and fossil content. Fossils and facies characteristics were described in thin sections from 182 samples used for sequence stratigraphy analyses. Abundance of green algae, gastropoda, bivalves, echinoderms, and non-skeletal grains (e.g., ooids, intraclasts, peloids, and aggregate grains) were considered. Sedimentologic textures and structures were considered qualitatively. Facies and microfacies types were mainly compared on the basis of the classical models provided by Wilson (1975) and Flugel (2010). For sequence stratigraphic interpretation, the concepts developed by many investigators (Emery and Myers, 1996; Catuneanu et al., 2005, 2009) were used. The combined use of facies and sedimentologic features (e.g. grain size, degree of sorting, grain composition and sedimentary structures) has resulted in high resolution correlations for the middle to late Devonian strata across the sections depression and provided a framework for interpretation of a detailed depositional environment. Sequences are defined as a conformable succession of genetically related strata, bound at the top and bottom by disconformities.

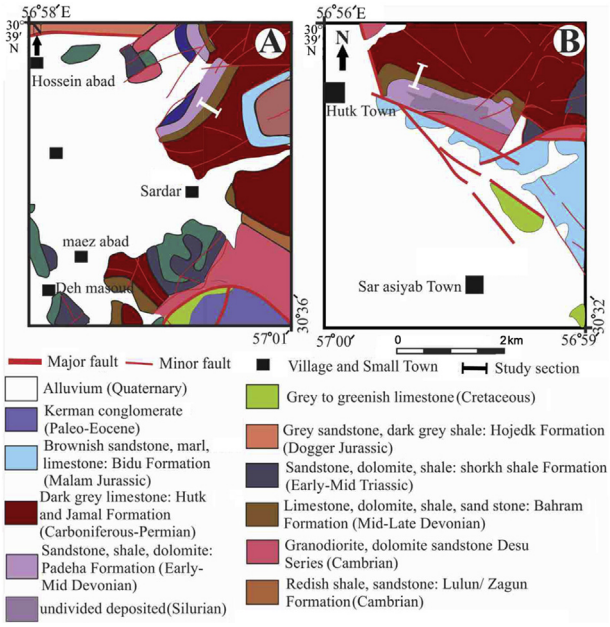

Figure 3. Simplified geological maps of the study areas with locations of the studied sections. (A) Sardar section, and (B) Hutk section sheet 1:100,000 of Zarand by Vahdati-Daneshmand et al. (1995), sheet 1:100,000.

4. Lithostratigraphy

The Bahram Formation in the sections conformably overlies the Padeha Formation with a transitional contact and underlies the Hutk Formation (equivalent to Shishto Formation) paraconformably. The hiatus which comprises a time span of up to 200 Ma can be explained by a widespread emersion (northwest Kerman) (Wendt et al., 2002). The conodont fauna collected in this section allows to assign a Givetian, Frasnian–late Famennian age to the Bahram Formation (Wendt et al., 2002). The Bahram Formation in both sections is dated as lower falsiovalis – upper marginifera zones (late Givetian–middle Famennian). Two new conodont species, Polygnathus jatalenti n. sp. ranging upper falsiovalis – lower hassi zones and P. chatrudensis with a range of upper hassi – linguiformis zones are erected. New age ranges of lower falsiovalis – upper rhenana zones and transitans – upper rhenana zones are proposed for P. zinaidae and P. alvenus. In the study area, the Bahram Formation is between 351 (Hutk) and 386 m (Sardar) thick, and generally includes limestone, sandstone, dolomite and shale units (Fig. 4). The rocks contain skeletal grains of various groups, including debris fossil and brachiopods which are very common together with coral, bryozoans, echinoderm, fish remains, gastropods, calcareous algae and bivalves. The rocks contain structures: ripple mark, cross bedding, mud crack, mud drapes, lamination, calcite veins and Scoyenia trace fossil. The followings are brief stratigraphic and lithological descriptions of study sequences which are summarized in Fig. 4.

5. Facies description and depositional environment

The Bahram Formation at the studied sections is subdivided into 14 different microfacies, each characterised by a depositional texture, petrographic analysis, skeletal and nonskeletal components. The general environmental interpretations of the microfacies are discussed in the following paragraphs. Based on paleoenvironmental and sedimentological analysis, 5 facies belts can be recognized: detrital facies (shore and mud flat) and carbonate facies (tidal flat, lagoon, shoal and shallow open marine).

5.1. Shore environment

5.1.1. Quartzarenite facies

Quartz is the dominating framework grain in the studied thin sections (Fig. 5A). The quartz grains are mostly monocrystalline. Recycled micritic grains are moderately sorted, with a grain-supported texture, set in calcite spar (Fig. 5B). The high compositional and textural maturity in the Bahram Formation quartzarenite, as well as trough and planar cross-bedding, ripple marks that are symmetric, laminations and scoyenia trace fossil indicate a high energy depositional environment for this facies (Fig. 5D–H). Asymmetrical of ripple marks are known to be characteristic of a coastal environment (Longhitano et al., 2012). Vertical grading of the quartzarenite to lithic sandstone, cross-bedding, and a vertical association of the clastic facies with carbonate tidal facies point to sedimentation in a shallow supratidal to an upper intertidal (foreshore to shoreface) environment (Flugel, 2010). In general, fining upward cycles of sandstone with features such as wavy and interference ripple marks and cross-bedding show that the petrofacies in the studied area was deposited in a costal environment (Chakraborty and Sensarma, 2008).

5.1.2. Sublitharenite facies

This petrofacies is brown to light-brown, thin to medium bedded, fine to medium grained, sub-rounded, submature to mature (high quartz) sandstone. It consists of sedimentary lithic, feldspar, muscovite and >80% quartz, with carbonate and ferruginous cement and about 3% matrix (Fig. 5C). The main characteristic of this lithofacies observed is the presence of planar cross-bedding and herringbone (Fig. 5G, J). Mud drapes were observed between many sandstone layers (Fig. 5K). The association of this facies suggests that deposition took place in shallow waters and at a different energy level (offshore) (Kostic et al., 2005). The presence of herringbone structures indicates that this facies was deposited in a fluctuating current direction setting, most likely tidal flat, especially intertidal setting (Strand, 2005; Folkestad and Satur, 2008).

5.1.3. Shale facies

Shale layers show thickness of less than 1 m and are intercalated with carbonates and sandstones (Fig. 5L). There is typically a delicate and visible lamination in which individual lamina is characterized by normal grading and an erosional base. The shales show two different colors including light brown fissile with horizontal lamination (siltysand) and grey to dark grey shale-form (Fig. 5H). Laminated shale contains very fine to fine, angular to sub-angular quartz grains, clay lamina and bioclastic debris. Fine quartz grains are abundant (<10%) in some parts silty form in sandy shale. The calcareous shales form (Fig. 5L) includes bioclastic debris, mud cracks and bioturbation (Fig. 5I). Fine to medium grained quartz, bioclastic debris and bioturbations in shale form show normal marine condition in a lower shoreface environment (such as mud flat). The grain size, bioturbation and bioclastic debris indicate that the light brown and gray shales were deposited in a low energy marine setting in an intermediate continental-marine environment (Warren, 2006). Mud crack sediment deposited in a costal environment or tidal flat setting (Warren, 2006). Also the bioturbated shales that are intercalated with sandstones indicate mixed mud-sand tidal flat deposition (Reineck and Singh, 1975).

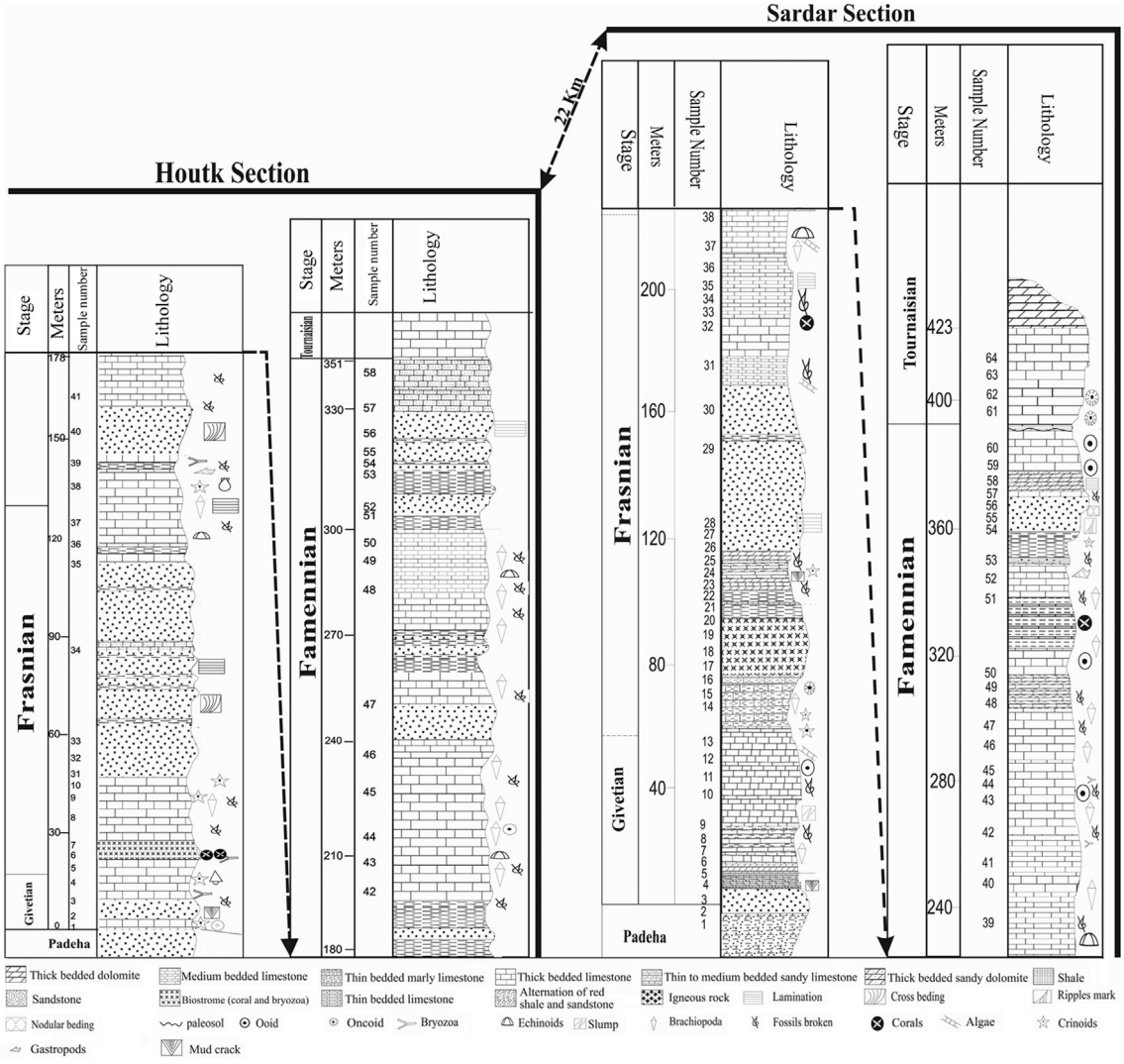

Figure 4. Stratigraphic sequence and rock components of studied succession in the Hutk and Sardar sections (according to field observation).

5.2. Tidal flat environment

5.2.1. Sandy bioclastic grainstone microfacies

The sandy bioclastic grainstone consists of medium-bedded, light gray, partially fossiliferous beds. The fauna includes brachiopod, echinoderm and bivalve debris. Fine- to medium-grained, poorly sorted, angular to subrounded, monocrystalline quartz is also present (approximately 15%). The allochems are cemented by a blocky and drusy sparite (Fig. 6A). This facies occurs at the base and top of the Bahram Formation, and it marks the beginning of its carbonate deposition. Given the presence of the sand-sized quartz minerals and the lack of micrite, it appears that the sandy bioclastic grainstone was formed in a high energy environment in tidal channels (Shinn, 1983, 1986).

5.2.2. Sandy dolomitized mudstone microfacies

This facies is thin to medium bedded dolomicrite with detrital grains (about 15% sub-rounded quartz). Its carbonate matrix (micrite) has suffered neomorphism and dolomitization. Main features of this facies include sand-sized detrital quartz, bird eyes fabric, calcite veins and dolomitization also low diversity of fossils. Sometimes dolomitization has led to obscuring primary textures of the rocks (Fig. 6B, C). Also there are skeletal fragments of brachiopods and crinoids (about ~5% of a total allochems) (Fig. 6D). These features and association with shallow facies (sandstone, shale and lagoon facies) demonstrate deposition in tidal flat and supratidal environments (Tucker, 2001; Bodzioch, 2003; Flugel, 2010). High amounts of micrites demonstrate a low energy in environment (Adachi et al., 2004). The dolomitized micrite and dolomudstone with fenestral were deposited in upper intertidal environments and according to Flugel (2010), sediments composed of a mixture of carbonate and siliciclastic sediments are common in near-coast and inner-shelf settings as well as at high latitudes (Palma et al., 2007). Dolomitization in this facies indicates depositions close to tidal flat (Lasemi et al., 2008).

5.3. Lagoon environment

5.3.1. Pelloid bioclastic packstone microfacies

This facies consists of gray, medium to thick beds of a peloid bioclast packstone. Peloids (40%) are the most abundant components in this microfacies and most peloids are uniform in size (Fig. 6E). The skeletal debris forms 30% of this facies and consists of echinoderms, brachiopods and algae. All the allochems are cemented by several generation by sparry calsit however the

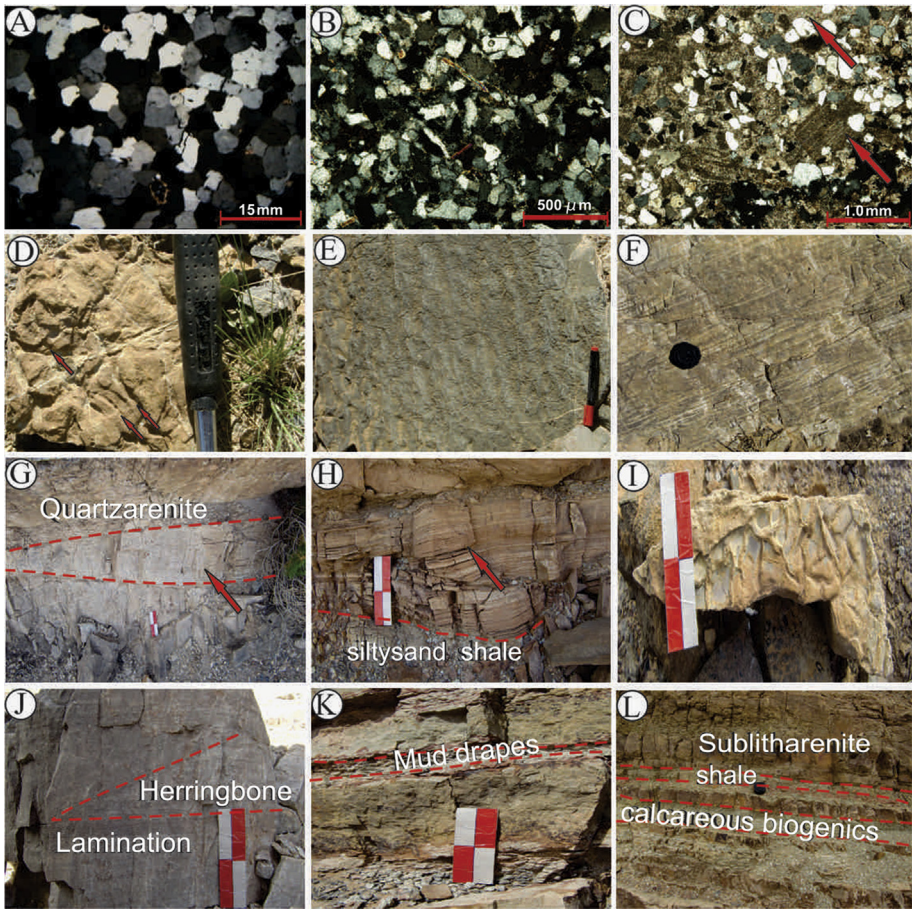

Figure 5. (A) Photomicrograph quartzarenite petrofacies with quartz grain, XPL; (B) photomicrograph quartzarenite petrofacies that is cemented by dolomite, XPL; (C) photomicrograph sublitharenite with feldspar and muscovite grain (arrows) and cement dolomite, XPL; (D) Scoyenia trace fossil (arrows) between sandstone beds; (E) wavy ripples in the quartzarenite; (F) succession quartzarenite with planar cross-bedding; (G) succession of trough cross-bedding (arrows) in the sublitharenite; (H) beds of horizontal and laminated sandstone (arrows) overlie succession shale; (I) beds with mud cracks in facies association; (J) succession of sandstone (herringbone cross-bedding and lamination); (K) mud drapes (arrows) between sandstone beds; (L) succession alternation shale and sandstone.

matrix is mainly micrite. This facies is distinguished by the abundance of pellet (maximum size 1 mm) and pelloids. This microfacies is interpreted to be located in the outer facies of a lagoon. In peloidal packstones, the presence of bioclasts and dominance of peloids indicate deposition in a low energy, shallow lagoonal environment with poor connection with the open marine (Tomasovych, 2004) and the low variety of fossils demonstrate deposition in enclosed shallow subtidal environment with low sedimentation rate (Tucker and Wright, 1990; Tucker, 2001; Flugel, 2010).

5.3.2. Bioclastic Umbellina (Calcareous algae) wackestone microfacies

The bioclastic wackestone consists of thin- to medium-bedded, light to dark gray beds of skeletal debris cemented by a micrite. The sparse skeletal fragments include crinoid stems and brachiopods, Umbellina algae (about 35%) and less than 5% debris fossil are minor grains (Fig. 6F). The skeletal grains are relatively intact (Fig. 6F). The skeletal grains have commonly micritized boundaries that show evidence of boring by algae (Flugel, 2010). The relatively low diversity and low abundance normal marine fauna, in the bioclast wackestone suggest the deposition was in a quiet water and lagoonal environment (Wilson, 1975; Hine, 1977; Nichols, 2000). This facies was deposited mainly in a sheltered lagoon environment with an open marine circulation under a low to moderate energy near shoals. The features of mentioned microfacies such as the lagoonal existence of gastropods, Umbellina algae and small brachiopods in micrite are indicative low energy environment (Bachmann and Hirsch, 2006; Husince and Sokac, 2006; Palma et al., 2007).

5.4. Shoal (barrier) environment

5.4.1. Coral framestone microfacies

This facies is composed of tabulte, rugose coral in, massive and domal colonies. Large coral fragments and bryozoanc are the main components. Subordinate components include crinoid debris. The degree of fragmentation and micritization in the fossils is relatively high and cavities of corals are filled by secondary dolomite and ferruginous cements (Fig. 7A–C). Textural features, stratigraphic relationship and the reworked characteristics of the coral fragments suggest that this microfacies formed in an upper slope environment under low- to medium-energy. Fragmentation indicates high energy, but dominance of micrite indicates that the high level of energy was not constant. Encrustations by corals and bryozoans probably occurred during calm phases (Kershaw and Brunton, 1999). The substratum was hard, appropriate for the attachment of diverse colonial organisms (Brett, 1988). This microfacies is interpreted to have been formed by in situ organisms as an organic reef (Wendt et al., 2002) and their few lateral

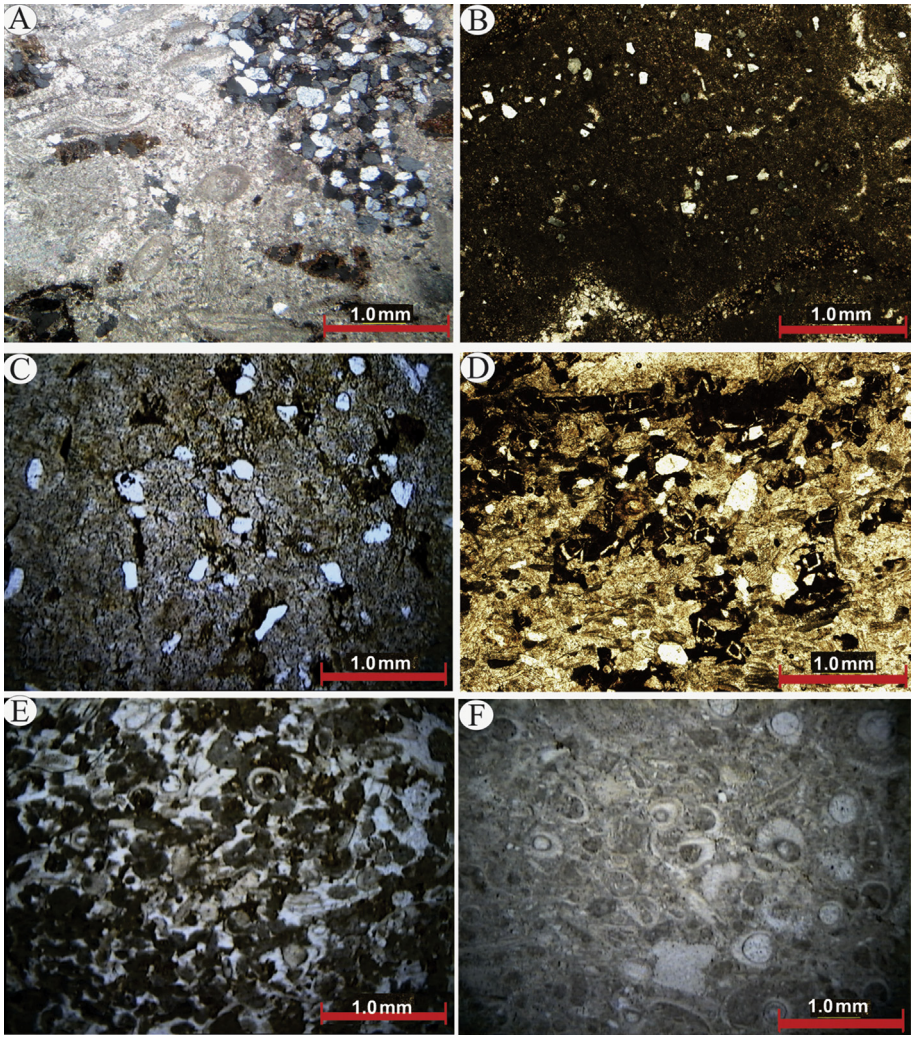

Figure 6. Photomicrograph showing (A) sandy bioclastic grainstone, XPL; (B) sandy dolomitized mudstone with fenestral fabric, XPL; (C, D) sandy dolomitized mudstone with grain quartz and dolomitization, XPL; (E) pelloid bioclastic wackestone/packstone, XPL; (F) bioclastic umbellina wackstone, PPL.

spreaded may indicate probably a patch reef in initial stages of development, affected by episodic storms and deposited in a shallow open marine shelf.

5.4.2. Ooid bioclastic grainstone microfacies

This facies is dark, medium bedded limestone. The predominant grain types are ooids and skeletal fragments. Biotic grain types include crinoids, brachiopods and gastropods. These grains are spherical, less structure and well sorted. Ooid nuclei consist of recrystallized shell fragments. Ooids have been influenced dolomitization and hematitization (Fig. 7D, H). To create ooids, it is required a saline and energetic environment (Tucker et al., 1993; Flugel, 2010). The features of this facies indicate moderate to high energy shallow waters with much movement and reworking of bioclasts and the production of ooids. Present bioclasts, ooids with tangential structures in this facies indicate a high energy environment that has been subjected to constant wave agitation and produced a well sorted grainstone (Tucker and Wright, 1990; Flugel, 2010) and cements demonstrate deposit on high energy environments of a seaward shoal within the surf zone (Wilson, 1975; Palma et al., 2007; Reolid et al., 2007; Adabi et al., 2010; Flugel, 2010) such energetic deposits mostly spread as barriers on carbonate platforms (Van Buchem et al., 2002).

5.4.3. Intraclastic bioclastic grainstone microfacies

This facies forms thick-bedded, light to medium gray beds composed of moderately sorted intraclasts (25%) and bioclasts (20%) that are surrounded by a sparite cement (Fig. 7E). Intraclasts are generally polymodal in size, ranging from 0.5 to 4 mm, with an average of 2.5 mm. Most of the intraclasts are subangular to angular. Some intraclasts are internally homogeneous and consist of micrites, while others display internal compositions such as pelloids and fossils. Bioclasts of algae, brachiopod and coral debris are present. All the allochems are cemented by sparite. Intraclast grainstones are often interpreted as deposits formed by storm wave erosion, tidal currents and reworking of various sediment types occurring in shallow-marine environments (Flugel, 2010). Roundness of intraclasts and the presence of sparite cement indicate depositition in high energy environments of erosive tidal channels of barriers (Tucker and Wright, 1990) that connect at lagoonal with open marine environment. The coarse and whole grains of the intraclasts and grainstone suggest that this facies was a leeward shoal.

5.4.4. Ooid grainstone microfacies

This microfacies type is less prominent in samples from the Hutk section. The grains consist of different components such as

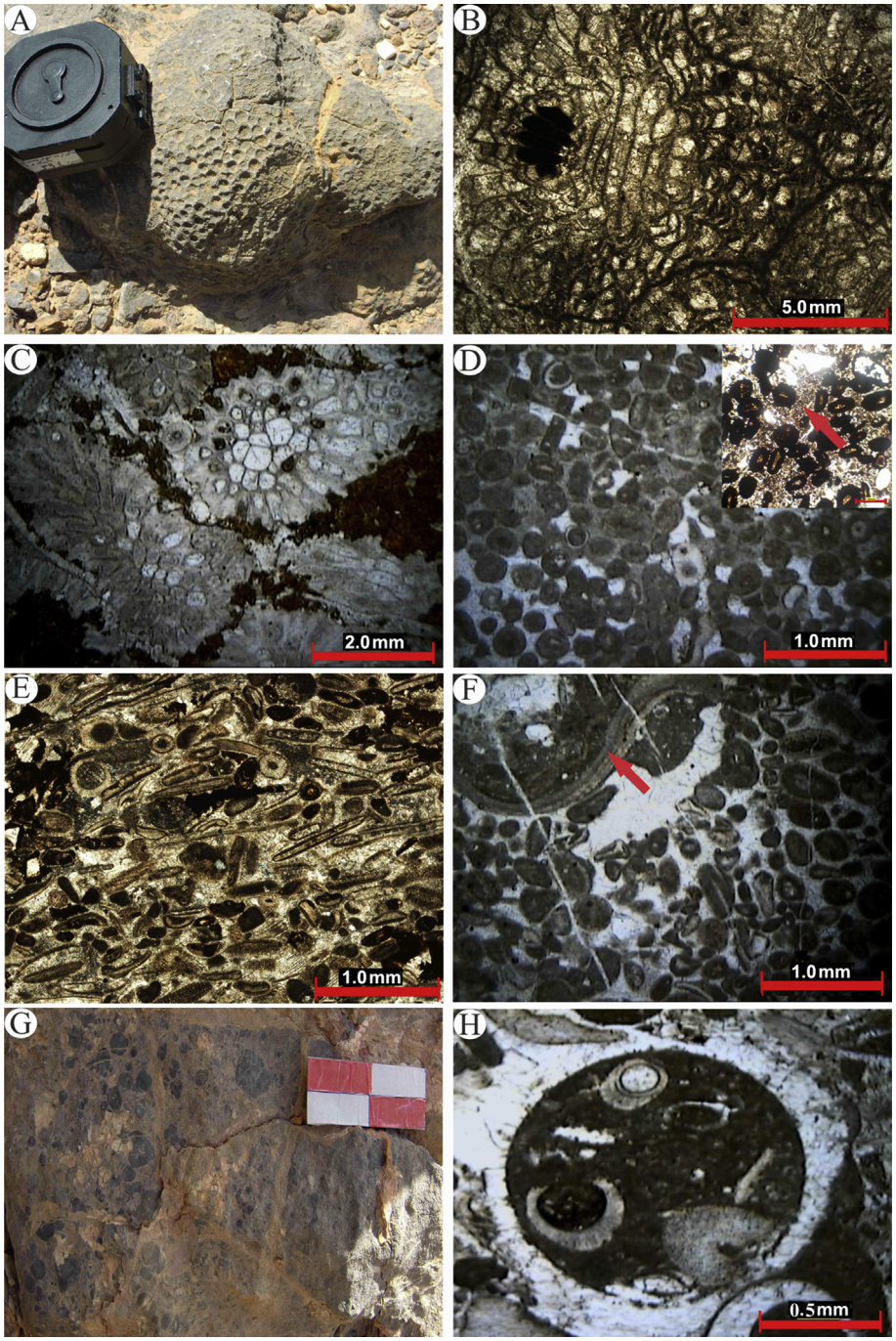

Figure 7. (A) Coral between succession coral boundestone microfacies; (B) photomicrograph coral boundestone microfacies, XPL; (C) bryozoa between coral boundestone microfacies, XPL; (D) photomicrograph of ooids and bioclast grain in the ooid bioclastic grainstone microfacies that is cemented by dolomitization and hematization (arrows), XPL; (E) photomicrograph intraclast bioclastic grainstone microfacies, XPL; (F) photomicrograph ooid grainstone, aggregate (arrows) upper picture, PPL; (G) aggregate grain in the succession limestone; (H) photomicrograph ooid grain with contains debris fossil, PPL.

ooids and algae (Fig. 7F, G). This facies consists of thick-bedded, fine- to coarse-grained ooid grainstone. The well-sorted ooids form 80% of this facies with less than 10% non-coated skeletal debris present. Grainstone texture, concentric ooids, and well-sorted components in these facies are indicators of high energy environment (Reolid et al., 2007). Such high energy deposits are typically associated with carbonate shoals and bars on or near the seaward edge of platforms (Wilson, 1975; Van Buchem et al., 2002; Flugel, 2010). The ooid grainstone represents shallowing-upward upper ramp shoals (Read, 1985).

5.5. Shallow open marine environment

5.5.1. Phosphatic packstone/grainstone microfacies

This microfacies is brown, thin bedded limestone (Fig. 8C). The predominant grain in this microfacies is phosphorite (20%). Major element geochemistry of the phosphorite samples (Table 1) shows that the amount of phosphorite is large. This microfacies is made up of alternations of fine to coarse phosphorite packstone and grainstone and small amounts of debris fossil and bryozans in spar (Fig. 8A, B). Well rounded quartz grains amounting to <5% are

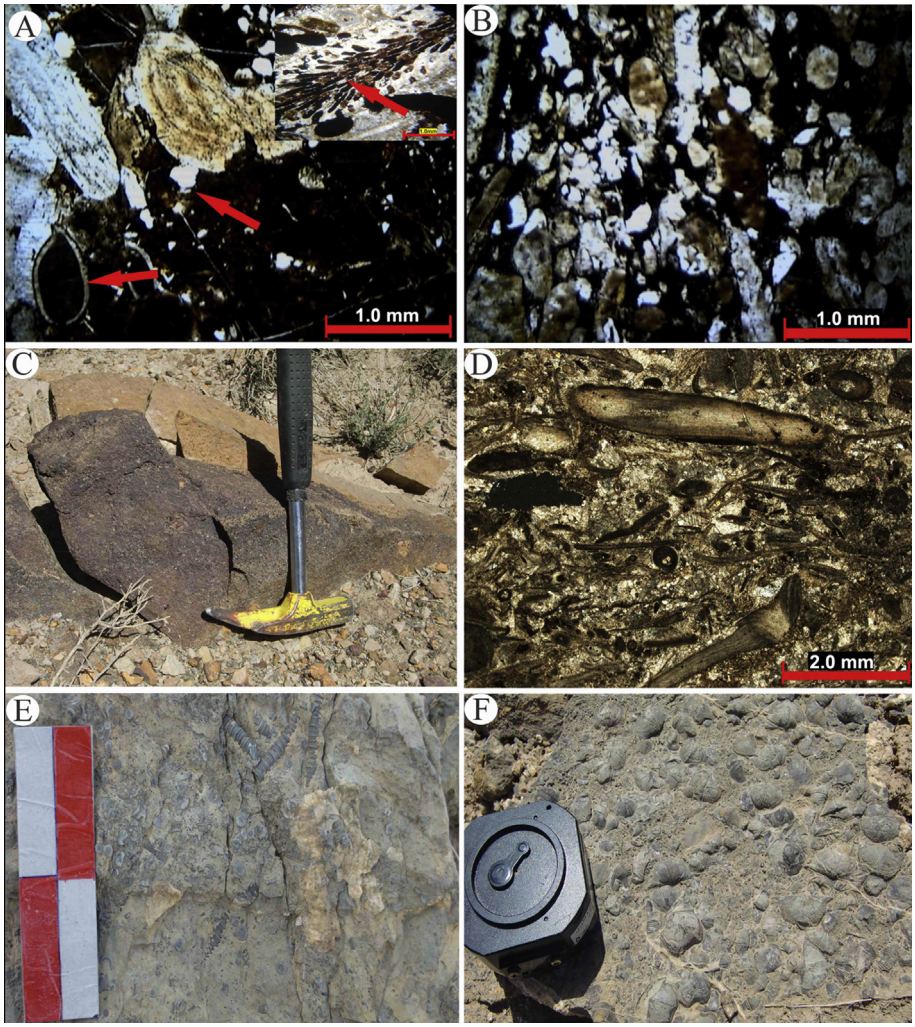

Figure 8. (A) Photomicrograph showing fossil and quartz grain that is cemented phosphorite, XPL; (B) photomicrograph phosphorite packstone/grainstone microfacies, XPL; (C) thin bedded containing phosphorite and debris fossil; (D) photomicrograph bioclastic packstone/wackstone, XPL; (E, F) succession limestone containing crinoid stem brachiopds abundant (bioclastic packstone/wackstone microfacies).

present. Fining upward cycles of carbonate facies with intercalations of deep open marine facies has been well-documented in the lower depositional sequence of Bahram Formation. Fossil debris in the microfacies association indicates seaward shoal to open marine setting. Intercalation of shale with thin bedded, phosphorite bearing limestones confirms shallow open marine environment with upwelling (Cook and Shergold, 1986; Frohlich, 2003). In phosphorite limestone intercalations, placoderm remains are locally abundant, and maybe phosphorite composition of this microfacies reflects secretion by fish under conditions of excess dissolved reactive phosphorus in the water column that was most likely associated with upwelling and cooler-water conditions on the shelf during maximum transgression (Katherine et al., 2002).

5.5.2. Bioclastic packstone/wackestone microfacies

This microfacies is consisted of colored cream, thick bedded limestone. These sediments contain brachiopods, echinoida, bryozoa, bivalves, gastropod and shell fragments (Fig. 8D–F). No sedimentary features indicative of shallow water or high energy sedimentation were observed. The lime-mud dominated lithology, presence of bioclasts and stratigraphic position indicate that deposition took place in a low energy shallow water environment below storm wave base (Corda and Brandano, 2003). Fabric and size of its skeletal grains and their similarity to bioclasts of barrier facies indicate an open marine position close to barion below seaward barrier. Presence of micrite and lack of detrital grains demonstrate to deposit it under wave base and conditions of a low energy

Table 1
Major oxide values (wt.%) of the selected limestone samples of the Bahram Formation in several thicknesses.

Section	Thickness (m)	SiO_2	Al_2O_3	BaO	CaO	Fe_2O_3	K_2O	MgO	MnO	Na_2O	P_2O_5	SO_3	TiO_2	LIO
Sardar	98	12.05	1.41	0.05	46.30	3.37	0.17	0.35	0.05	0.32	17.50	0.68	0.13	17.49
Sardar	300	10.02	0.75	0.04	47.04	3.52	0.21	0.42	0.07	0.28	19.85	0.92	0.17	16.7
Sardar	305	36.56	2.14	0.05	29.19	4.96	0.38	1.56	0.05	0.47	17.04	0.77	0.24	6.55
Hutk	28	17.5	1.02	0.08	39.8	4.7	0.25	0.30	0.02	0.45	17.98	0.50	0.10	16.4
Hutk	235	29.01	5.2	0.12	24.8	7.01	0.02	3.7	0.35	0.52	17.80	1.01	0.28	10.02

environment. Variety and size of bioclasts indicate deposition in shallow open marine setting (Spalletti et al., 2001).

6. Sedimentary model

Facies models represent comprehensive summaries of processes within sedimentary environments that can be obtained from evidence of modern and ancient facies (Walker, 2006). Due to their well-defined palaeoecological requirements, they represent valuable facies indicators (Rasser et al., 2005). Palaeogeographic maps of the late Ordovician to late Devonian of northern Arabia suggest that north Africa and Arabia formed a broad stable continental shelf on the northern margin of the Gondwana supercontinent (Husseini, 1991; Sharland et al., 2001; Wendt et al., 2002, 2005; Golonka, 2007; Ruban et al., 2007; Torsvik and Cocks, 2009; Domeier and Torsvik, 2014) bordering the Paleo-Tethys ocean (Fig. 9A, B). Bahram Formation (middle–late Devonian) times a relative rise of sea level flooded the pre-existing carbonate platforms and surrounding siliciclastic shelves (Wendt et al., 2002) (Fig. 9B). After a long period of near shore and intertidal conditions during the early and early middle Devonian (Padeha Formation), the onset of open marine conditions appears diachronous (Wendt et al., 2002). According to the Devonian paleogeography of Iran (Sharland et al., 2001; Wendt et al., 2002, 2005; Ruban et al., 2007; Domeier and Torsvik, 2014), the sediments of the Bahram Formation were deposited in a divergent passive margin setting at the southern margin of Paleotethys Ocean (Domeier and Torsvik, 2014). The opening of this ocean (rift basin) can be traced to the Silurian time, and the rift basin was converted to stable passive margin in the Devonian time (Berberian and King, 1981). Facies patterns and sedimentary environments north of Kerman indicate a carbonate platform and a shallow open marine embayment during the late middle–late Devonian (Wendt et al., 2002) (Fig. 9C, D). Wendt and his coworkers (2002) divided Bahram Formation palaeogeography into three part in the north of Kerman (Fig. 9C). All the studied sections of this study are zone shallow open marine. The recognized microfacies have allowed the differentiation of several carbonate-clastic marine system environments including supratidal shoreline (with mud flat), tidal flat, lagoon, shoal and shallow open marine environments (Fig. 9D). Terigenous rocks with features such as ripple marks, herringbone and cross-bedding in most sandstone facies association with mature sandstone petrofacies and primary fine crystal dolomite show that they were deposited in a costal environment or tidal flat setting. Mud cracks (in shale facies) and Scoyenia trace fossils are commonly related to the supratidal and upper intertidal zones. The reef builders are partly in place, partly overturned and accumulated, probably by storm events (Wendt et al., 2002). The platform margin is represented by ooid and bioclast grainstone. Ooid and bioclast grainstone is interpreted to represent a shoal in a shallow subtidal zone, characterized by the winnowing of coarse-grained and sorted ooid and bioclast fragments. The predominantly coarse and well-sorted allochems indicate deposition in a well-circulated environment in a shallow subtidal zone (Schulze et al., 2005). High energy shoal facies belt formed a barrier at the platform margin and protected a very wide lagoon. The presences of peloids and algae allochem, high energy shoal facies, protected lagoon, are all evidence of deposition on a broad carbonate-clastic shelf (Schlager, 2005; Flugel, 2010). The shallow open marine is represented by copious bioclastic (brachiopod, crinoid) packstone. The predominantly phosphorite indicates deposition in an open marine during the upwelling. The occurrences of diverse skeletal grains, abundant ooids, peloids and some intraclasts and early diagenetic dolomites in the Bahram limestone are similar to those in modern, tropical, shallow-marine

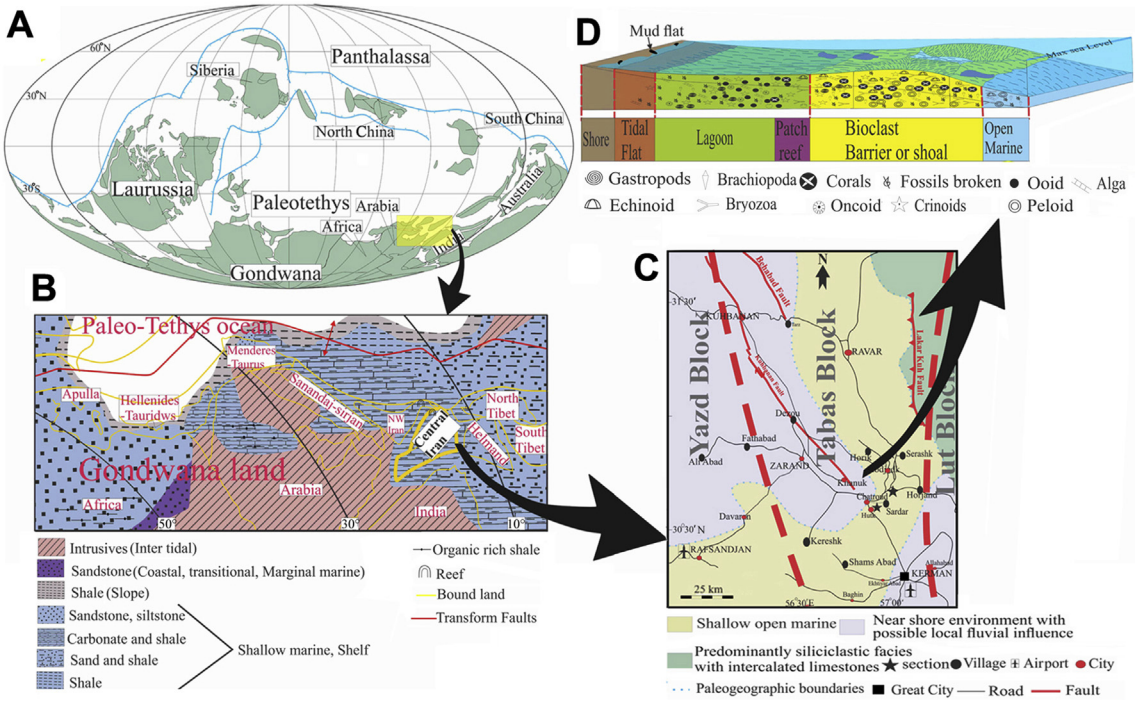

Figure 9. Paleogeographic map of central Iran during the late Devonian. (A) Paleogeographic reconstruction showing simplified plate boundaries and Iran location of Gondwana land (Domeier and Torsvik, 2014); (B) close-up view of yellow square of Fig. 9A. Paleo-tectonic, paleogeographic and lithology map of the north Gondwana land and central Iran plates during the late Devonian (modified from Golonka, 2007; Ruban et al., 2007; Torsvik and Cocks, 2013). The central Iran is shown with chromatic line; (C) paleogeographic map of north Kerman during the upper Givetian to Famennian (modified form Wendt et al., 2002); (D) schematic block diagram for depositional model of the Bahram Formation in the study area with available allochem in facies belt.

waters (Lees, 1975). During deposition of the Bahram Formation a shallow open marine environment was established as documented by skeletal limestones, sandstones, dolomites and shales (Fig. 9D).

7. Sequence stratigraphy

Sequence stratigraphy defines depositional systems and surfaces related to change of eustatic sea level. The sedimentary facies characteristics of the Bahram Formation show a distinctive number of sequence boundaries, systems tracts and depositional sequences. We constructed a sequence stratigraphy for the studied sections based on standard classification of Catuneanu et al. (2005, 2009) that considered four standard 3rd-order (Vail et al., 1977) system tracts (LST, TST, HST, FSST). Bahram Formation has been deposited in the upper and lower Kaskaskia Mega sequence (Gradstein et al., 2004). In the description of sections, deepening trends are considered to be a transgressive system tract (TST), shallowing trends are interpreted as a highstand system tract (HST), the change from deepening towards shallowing is interpreted as maximum flooding surface (mfs). During the early and early middle Devonian near shore and intertidal conditions afterward the onset of open marine conditions appears diachronously (transgressive) (Wendt et al., 2002), therefore more carbonate sediments were supplied to the sedimentary basin (southern margin of the Paleo-thetys Ocean or northern parts of the Gondwana land). The facies distribution, stratal patterns and sequence boundaries permit the identification of four separate 3rd-order depositional sequences and the sequences that occurred during of the late Givetian, Frasnian and Famennian time (Fig. 10). In the present study, the Devonian Bahram Formation is regarded as a megasequence (Kaskaskia Cycle) based on the world cratonic models (Sloss and Speed, 1974). The regional correlation of the upper Palaeozoic successions (Fig. 2) in Iran and neighboring countries shows for the studied-formations that Juban Formation in Saudi Arabia, Kuwait (partly), Chalki volcanics, Pirispiki, Kaista and part of Ora formations in Iraq, the Yeginili Pendik and Buykecell formations in Turkey, Khoshyilagh Formation in Alborz Iran and parts of Muli and Zakeen formations in NW and South of Iran (Zagros) respectively (Sharland et al., 2001).

7.1. Sequence 1

Sequence 1 represents the near shore deposition of the Bahram Formation which overlies the continental sandstone of the middle Devonian Padeha Formation. The lower boundary of the first sequence is marked (SBI) at the sandy dolomitized mudstone which contains one mud crack (Bahram Formation) at the top of the sandstone and conglomerate (Padeha Formation) in the studied sections. There is an unconformity (SBI) developed between the Padeha (continental rock sandstone and conglomerate) and Bahram Formation. Therefore, it is interpreted as a (SB) sequence boundary Type-1 at the base of sequence 1. The sequence 1 in the lower part of the Bahram Formation is classified into lowstand systems tract (LST), transgressive systems tract (TST) and highstand systems tracts (HST) (Fig. 10). The basal part of sequence 1 predominately consists of tidal flat lagoon and shoal facies. This sequence begins with ferruginous sandy dolomites limestone, and shale as a lowstand systems tract (LST). The onset of fossiliferous limestone with coral, crinoid and whole echinoderms represents the transgressive surface (TS) and the beginning of the transgressive systems tract (TST). The maximum flooding surface (MFS) of sequence 1 is represented by limestone and shale that are very rich in phosphorite (Fig. 10). Phosphorite was most likely associated with upwelling and cooler-water conditions on the shelf during maximum transgression (Katherine et al., 2002). The highstand systems tracts (HST) of this sequence are dominated by limestone and sandstone (Tidal flat and shore facies). Thickness of sequence 1 varies between 115 m in Hutk and 170 m in Sardar sections (Fig. 11). Its age is Givetian and Frasnian. The early highstand systems tract in Hutk section is characterized by a proliferation of grain-supported shoal facies (such as ooid bioclastic grainstone). This part mainly comprises the shoal and tidal flat facies association. The upper part of sequence 1 (late HST) indicates upward shallowing trend. Progradation of siliciclastic into late HST is inferred by sandy bioclastic grainstone and ooid bioclastic grainstone overlain by sandstone and sandy dolomitized mudstone bearing fenestral facies (Fig. 10). The shallowing-upward trend from shore is indicative of a progradational stacking pattern during the highstand systems tract (Kwon et al., 2006).

7.2. Sequence 2

This sequence has a thickness of about 75 m (Hutk) and 102 m (Sardar). The type 1 basal sequence boundary is marked by fenestral dolomudstone and mud cracked shale facies. Dolomitized supratidal deposits with dissolution features, fenestrate and mud cracks indicate subaerial exposure (Catuneanu et al., 2005). Therefore, it is interpreted as a SBI sequence boundary at the base of sequence 2. The LST sediments of this sequence include pelloid and bioclastic limestone deposits, which are deposited in tidal flat and lagoon settings. The TS surface is located in the basal part of the pelloid and bioclastic wackstone deposits. The part of the sequence

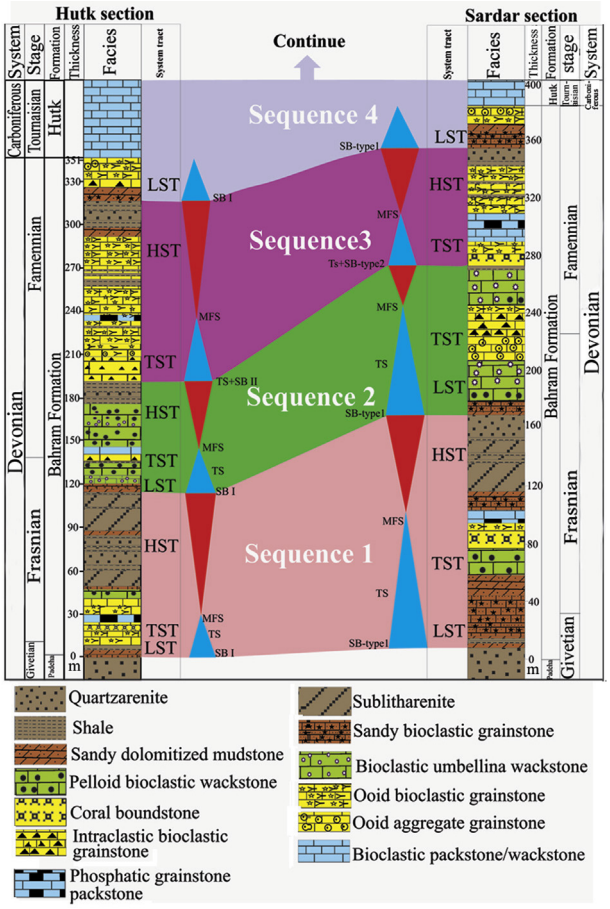

Figure 10. Facies and sequence stratigraphy correlation chart of Hutk and Sardar sections. The recorded four sequence boundaries and depositional sequences are illustrated.

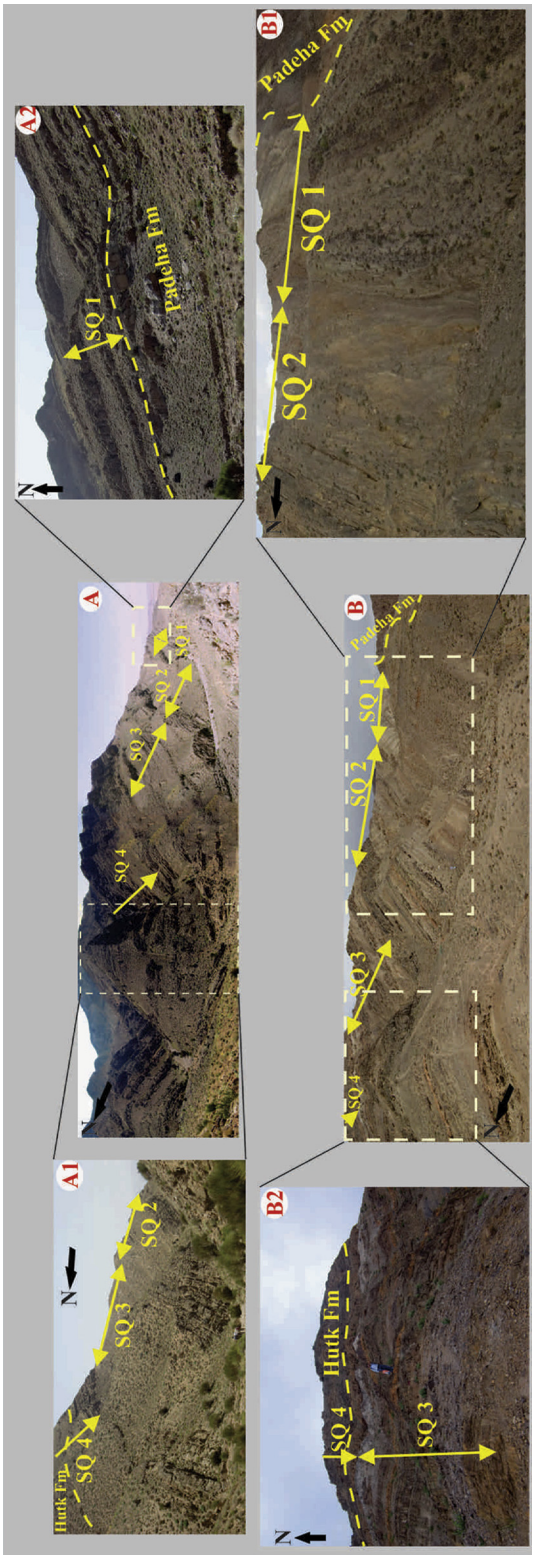

Figure 11. (A) Panoramic photo of the Sardar section and four depositional sequences; (A1) close-up view of sequence 1; (A2) close-up view of sequence 2, 3, 4 and top Baram Formation; (B) panoramic photo of the Hutk section and four depositional sequences; (B1) close-up view of sequence 1 and lower Bahram Formation; (B2) close-up view of sequence 2, 3, 4 and top Baram Formation.

1 (TST) consists of different shoal facies [such as ooid aggregate grainstone, ooid bioclastic grainstone (only Sardar section) and intraclast bioclastic grainstone facies] and shows a deepening upward unit. Maximum flooding surface located at the tops of the TST corresponds to a shift with associated open marine facies (Fig. 10). Bioclastic wackestone with abundant brachiopod debris represents deep-water facies and is interpreted as the MFS. Sediments that overlie the MFS mainly consist of lagoon, with thin intervals of shore facies (HST). The late HST shows a trend toward more protected sediments (pelloid bioclastic wackstone with major umbellina algae), expressing a filling of the accommodation space. The highstand systems tract (HST) comprises alternations of lagoon facies and shallow marine facies. The uppermost interval of this systems tract shows sandy shale lithology that is used to detect the sequence boundary. These sediments are interpreted as the HST. The HST shows a trend toward more protected sediments, expressing filling of the accommodation space. The depositional sequence 2 formed during the late Frasnian–Famennian.

7.3. Sequence 3

The boundary between sequence 2 and 3 is associated with shoreface that shows no clear evidence of sudden falling of sea level. Rapid fall of relative sea level caused the formation of composite sequence boundary (TS + SB type 2) at the base of the TST sediments. This sequence is 125 m (Hutk section) and 82 m (Sardar section) thick and its microfacies association can grouped into transgressive and highstand systems tracts. The lower part of sequence 1 (TST) is characterized by ooid bioclastic grainstone and coral boundstone (only in Sardar section) with intercalated shale. The MFS is marked by a phosphorite rich marine microfacies and separates TST from HST. Seem an ooid bioclastic grainstone with superabundant bryozoans and crinoids overlies the MFS. These sediments are interpreted as the early HST, which deposits are mostly composed of shoal microfacies. Inter bedded shoal deposits with alternation of calcareous shale indicate late HST deposits. The late HST shows a trend toward increased sedimentation (shoal and shallow facies), expressing a filling of the accommodation space. The boundary between sequence 3 and sequence 4 is put at the top of a quartzarenite petrofacies (Fig. 11). In both sections, the upper boundary of the third depositional sequence is SB type 1 with the presence of Scoyenia ichnofacies in sandstone (10 cm) at Sardar section and quartzarenite facies (white quartarenite guideline layers in observation field) at the Hutk section. This sequence is late Famennian in age and increasing sediment supply, resulting from shoal transgression, is recorded by the deposition of shoal sediments (TST). A long period of shoal conditions, reflecting a balanced situation between accommodation and sedimentation, characterizes the aggradational depositional pattern.

7.4. Sequence 4

The LST sediments of the fourth depositional sequence include tidal flat and shoal facies (in both sections). The sea level transgression caused the deposition of shallow subtidal facies within an aggradational stacking pattern in sections area. In addition to tidal flat and shoal deposition during the fall of sea level. These are interpreted as the lowstand systems tract (LST) of this sequence. The end of the LST sediments is placed at the top of the Bahram Formation, which is overlain by the carbonate deposits of the Hutk and Jamal formations (Carboniferous). An increase in 3rd-order accommodation space is indicated by shoal facies overlain by shallow-open marine facies. This sequence has been aged Famennian.

8. Conclusions

Generally, the lower Devonian and part of middle Devonian succession is absent in most part of the middle East, due to erosion during the Hercynian Orogeny (Wendt et al., 2002) but the basal part of Bahram Formation of latest Givetian age in the sections, transgressively overlies the top of Padeha Formation and continues to the Famennian. It conformably underlies the gray limestones and massive dolomites of early Carboniferous Hutk Formation. Bahram Formation in the north of Kerman basin mainly consists of carbonate-clastic (limestone, dolomite, sandstone, shales). 14 micro/petrofacies types dominated by matric, allochem and sedimentary structures were identified in the carbonates and clastics of the Bahram succession. The late Devonian part of the succession is the most different in the north of Kerman city (south Tabas block) (Wendt et al., 2002) with a dominance of siliciclastic deposits of shelf to shoreline environments. The other two sections are characterized by a mixed succession of carbonate siliciclastic shelf deposits. The sedimentation of the Bahram Formation took place on a shallow carbonate-siliciclastic mixed shelf setting, in a shelf facies belts consisting of shore, tidal flat, lagoon, barrier shoal and shallow open marine. The regional differentiation most likely reflects their position on separate tectonic blocks on which different facies conditions developed due to different tectonic movements. In accordance with the global trend, the middle Devonian to upper Devonian is uniformly dominated by the production of massive carbonates, mostly of reefoidal origin, although a thick intercalation of biolaminated carbonates in the study area records a long period of restricted extremely shallow-water conditions. The four upward-shallowing cycles recognized from the Bahram Formation are related to sea level variations. Three complete 3rd-order depositional sequences and one sequence joint with Hutk Formation in shallowing patterns were recognized in the studied formations. The predominant facies associations developed in formation demonstrate an overall transgression-regression cycle in the middle to late Devonian in the southern Tabas block.

Acknowledgments

This work is a part of project of the Hormozgan University and two master theses of the senior author, which is supported by the Department of Geology at Hormozgan University of Bandar Abbas, Iran. The authors are grateful to the University of Hormozgan for providing financial and technical support. We are grateful to reviewers, Prof. Jobst Wendt (Geoscience Universitat Tubingen, Germany) for his valuable guidance and staff of Geoscience Frontiers journal (especially Prof. Xiaoqiao Wan, Dr. Mudan Yin, and Dr. Lily Wang) for helpful comments, suggestions and editing of manuscript. Finally, we thank Mr. Amin Modie, Ali Hashmie, and Dr. Mohmmad Javad Hasanie for their contributions to this study, especially during field and laboratory work.

References

Adabi, M.H., Salehi, M.A., Ghabeishavi, A., 2010. Depositional environment, sequence stratigraphy and geochemistry of lower Cretaceous carbonates (Fahliyan Formation), south-west Iran. Journal of Asian Earth Sciences 39, 148–160.
Adachi, N., Ezaki, Y., Liu, J., 2004. The origins of peloids immediately after the end-permian extinction, Guizhou Province, South China. Sedimentary Geology 164, 161–178.
Al-Hajri, S.A., Filatoff, J., 1999. Stratigraphy and operational palynology of the Devonian system in Saudi Arabia. GeoArabia 4 (1), 53–68.
Al-Juboury, A.I., AL-Hadidy, A.H., 2009. Petrology and depositional evolution of the paleozoic rocks of Iraq. Marine and Petroleum Geology 26, 208–231.
Al-Sharhan, A.S., Nairn, A.E.M., 1997. Sedimentary Basins and Petroleum Geology of the Middle East. Elsevier, Amsterdam, p. 843.
Bachmann, M., Hirsch, F., 2006. Lower Cretaceous carbonate platform of the eastern Levant (Galilee and the Golan Heights): stratigraphy and second-order sea-level change. Cretaceous Research 27, 487–512.
Bahrami, A., Gholamalian, H., Corradini, C., Yazdi, M., 2011. Upper Devonian conodont biostratigraphy of Shams Abad section, Kerman Province, Iran. Rivistaltaliana di Paleontologia e Stratigraphia 117, 199–209.
Berberian, M., King, G.C.P., 1981. Toward a palaeogeography and tectonic evolution of Iran. Canadian Journal of Earth Sciences 18, 210–265.
Bodzioch, A., 2003. Calcite pseudomorphs after evaporates from the Muschelkalk (Middle Triassic) of thy Holy Cross Mountains (Poland). Geologos 7, 169–180.
Brett, C.E., 1988. Paleoecology and evolution of marine hard substrate communities: an overview. Palaios 3 (4), 374–378.
Brew, G., Barazangi, M., 2001. Tectonic and geologic evolution of Syria. GeoArabia 6 (4), 573–616.
Catuneanu, O., Abreu, V., Bhattacharya, J.P., Blum, M.D., Dalrymple, R.W., Eriksson, P.G., Fielding, C.R., Fisher, W.L., Galloway, W.E., Gibling, M.R., Giles, K.A., Holbrook, J.M., Jordan, R., Kendall, C.G.St.C., Macurda, B., Martinsen, O.J., Miall, A.D., Neal, J.E., Nummedal, D., Pomar, L., Posamentier, H.W., Pratt, B.R., Sarg, J.F., Shanley, K.W., Steel, R.J., Strasser, A., Tucker, M.E., Winker, C., 2009. Towards the standardization of sequence stratigraphy. Earth-Science Reviews 92, 1–33.
Catuneanu, O., Martins-Neto, M.A., Erikson, P.G., 2005. Precambrian sequence stratigraphy. Sedimentary Geology 176, 67–95.
Chakraborty, T., Sensarma, S., 2008. Shallow marine and coastal eolian quartzarenites in the Neoarchean–Palaeoproterozoic Karutola Formation, Dongargarh Volcano-sedimentary succession, central India. Precambrian Research 162, 284–301.
Cook, P.J., Shergold, J.H., 1986. Phophate Deposits of the World.1, Proterozoic and Cambrian Phosphorites. Cambridge University Press, Cambridge, p. 389.
Corda, L., Brandano, M., 2003. Aphotic zone carbonate production on a Miocene ramp, Central Apennines, Italy. Sedimentary Geology 161, 55–70.
Dastanpour, M., Bassett, M., 1998. Palaeozoic sequences in Kerman region. In: Mawson, R., Talent, J.A., Wilson, G. (Eds.), UNESCO_IGCP Project 421, North Gondwanan Mid-Palaeozoic Bioevent/biogeography Patterns in Relation to Crustal Dynamics, Esfahan Meeting (17-20 December, 1998). Shahid Bahonar University, Kerman, Iran, p. 21. Abstract book.
Domeier, M., Torsvik, T.H., 2014. Plate tectonics in the late Paleozoic. Geoscience Frontiers 5, 303–350.
Dorrik, A.V.S., 2010. Sedimentary Rocks in the Field: a Colour Guide, fifth ed. Manson Publishing Ltd, p. 320.
Dunham, R.J., 1962. Classification of carbonate rocks according to depositional texture. In: Ham, W.E. (Ed.), Classification of Carbonate Rocks. American Association of Petroleum Geologists Memoir 1, pp. 108–121.
Embry, A.F., Klovan, J.E., 1971. A late Devonian reef tract on Northeastern Banks Island, NWT. Bulletin of Canadian Petroleum Geology 19, 730–781.
Emery, D., Myers, K., 1996. Sequence Stratigraphy. Blackwell, Oxford, p. 297.
Flugel, E., 2010. Microfacies of Carbonate Rocks, Analysis, Interpretation and Application. Springer-Verlag, Berlin, p. 976.
Flugel, H., Ruttner, A., 1962. Vorbericht über paläontologisch-stratigraphische Untersuchungen im Paläozoikum von Ozbak-kuh (NE Iran). Geologischen Bundesanstalt 2, 146–150.
Folkestad, A., Satur, N., 2008. Regressive and transgressive cycles in a rift-basin: depositional model and sedimentary partitioning of the Middle Jurassic Hugin Formation, Southern Viking Graben, North Sea. Sedimentary Geology 207, 1–21.
Frohlich, S., 2003. Phosphatic black pebbles and nodules on a Devonian carbonate shelf (Anti-Atlas, Morocco). Journal of African Earth Sciences 12, 243–254.
Ghavidel-Syooki, M., 1994. Biostratigraphy and Paleo-biogeography of Some Paleozoic Rocks at Zagros and Alborz Mountains, Iran. Geology Survey Publication, Iran, p. 168.
Ghavidel-syooki, M., Mahdavian, M., 2010. Palynostratigraphy of Devonian strata in Hutak area, nothern Kerman Province. Stratigraphy and Sedimentology Researches 39, 19–32 (in Persain).
Gholamalian, H., 2003. Age implication of late Devonian conodonts from the Chahriseh area northeast of Esfahan, central Iran. Courier Forschungsinstitut Senckenberg 245, 201–207.
Gholamalian, H., 2007. Conodont biostratigraphy of the Frasnian-Famennian boundary in the Esfahan and Tabas areas, Central Iran. Geological Quarterly 51, 453–476.
Gholamalian, H., Ghorbani, M., Sajadi, S.H., 2009. Famennian conodonts from Kal-e-Sardar section, Eastern Tabas, Central Iran. Rivista Italiana di Paleontologia e Stratigrafia 115, 141–158.
Gholamalian, H., Kebriaei, M.R., 2008. Late Devonian conodonts from the Hojedk section, Kerman Province, Southeastern Iran. Rivista Italiana di Paleontologia e Stratigrafia 114, 171–181.
Golonka, J., 2007. Phanerozoic paleo environment and paleolithofacies maps: late Paleozoic. Geologia 66, 145–209.
Gradstein, F.M., Ogg, J.G., Smith, A.G., 2004. A Geologic Time Scale 2004. Cambridge University Press, Cambridge, p. 589.
Hine, A.C., 1977. Lily Bank, Bahamas: history of an active oolite sand shoal. Journal of Sedimentary Petrology 47, 1544–1581.
Huckriede, R., Kursten, M., Venzlaff, H., 1962. Zur Geologie des Gebietes zwischen Kerman und Saghand (Iran). Beibefte Geologisches Jahrbuch 51, 197.

Husince, A., Sokac, B., 2006. Early Cretaceous benthic associations (foraminifera and calcareous algae) of a shallow tropical-water platform environment (Mljet Island, southern Croatia). Cretaceous Research 27, 418–441.
Husseini, M.I., 1991. Tectonic and depositional model of the Arabian and adjoining plates during the Silurian-Devonian. American Association of Petroleum Geologists Bulletin 75, 108–120.
Katherine, A.G., McMillan, N.J., McCarson, B.L., 2002. Geochemical analysis and paleoecological implications of phosphatic microspherules (otoliths?) from Frasnian-Famennian boundary strata in the Great Basin, USA. Palaeogeography, Palaeoclimatology, Palaeoecology 181, 111–125.
Kershaw, S., Brunton, F.R., 1999. Paleozoic stromatoporoid taphonomy: ecologic and environmental significance. Palaeogeography, Palaeoclimatology, Palaeoecology 149, 313–328.
Kostic, B., Bech, A., Aigner, T., 2005. 3-D sedimentary architecture of a quaternary gravel delta (SW-Germany): implication for hydrostratigraphy. Sedimentary Geology 181, 143–171.
Kwon, Y.K., Chough, S.K., Choi, D.K., Lee, D.J., 2006. Sequence stratigraphy of the Taebeak group (Cambrian– Ordovician) Mideast Korea. Sedimentary Geology 192, 19–55.
Laboun, A.A., 2010. Paleozoic tectono-stratigraphic framework of the Arabian Peninsula. Journal of King Saud University (Science) 22, 41–50.
Lasemi, Y., Ghomashi, M., Amin-Rasouli, H., Kheradmand, A., 2008. The lower Triassic Sorkh shale formation of the Tabas block, east central Iran: succession of a failed-rift basin at the paleotethys margin. Carbonates and Evaporites 23, 21–38.
Lees, A., 1975. Possible influence of salinity and temperature on modern shelf carbonate sedimentation. Marine Geology 19, 159–198.
Longhitano, S.G., Mellere, D., Steel, R.J., Ainsworth, R.B., 2012. Tidal depositional systems in the rock record: a review and new insights. Sedimentary Geology 279, 2–22.
Morzadec, P., Dastanpour, M., Wright, A.J., 2002. Asteropygine trilobites from the late Devonian of the Kerman region, Iran. Alcheringa 26, 143–149.
Nichols, G., 2000. Sedimentology and Stratigraphy. Blackwell Science, Oxford, p. 355.
Palma, R.M., Lopez-Gomez, J., Piethe, R.D., 2007. Oxfordian ramp system (La Manga Formation) in the Bardas Blancas area (Mendoza Province) Neuquen Basin, Argentina: facies and depositional sequences. Sedimentary Geology 195, 113–134.
Pettijohn, F.J., Potter, P.E., Siever, R., 1987. Sand and Sandstone, second ed. Springer, New York, p. 553.
Rasser, M.W., Scheibner, C., Mutti, M., 2005. A paleoenvironmental standard section for Early Ilerdian tropical carbonate factories (Corbieres, France; Pyrenees, Spain). Facies 51, 217–232. http://dx.doi.org/10.1007/s10347-005-0070-9.
Read, J.F., 1985. Carbonate platform facies models. American Association of Petroleum Geologists 69, 1–21.
Reineck, H.E., Singh, I.B., 1975. Depositional Sedimentary Environments. Springer-Verlag, New York, p. 439.
Reolid, M., Gaillard, C., Lathuiliere, B., 2007. Microfacies, microtaphonomic traits and foraminiferal assemblages from upper jurassic oolitic-coral limestones: stratigraphic fluctuation in a shallowing-upward sequence (French jura, Middle Oxfordian). Facies 53, 553–574.
Ruban, D.A., Al-Husseini, M., Iwasaki, Y., 2007. Review of middle east paleozoic plate tectonics. GeoArabia 12, 35–56.
Ruttner, A.W., Nabavi, M.H., Hajian, J., 1968. Geology of the Shirgesht Area (Tabas Area, East Iran). Geological Survey of Iran, Reports 4, p. 133.
Schlager, W., 2005. Carbonate Sedimentology and Sequence Stratigraphy. SEPM (Society for Sedimentary Geology), Tulsa, Oklahoma, USA, p. 208.
Schulze, F., Kuss, J., Marzouk, A., 2005. Platform configuration, microfacies and cyclicities of the upper Albian to Turonian of west-central Jordan. Facies 50, 505–527.
Scotese, C.R., Mckerrow, W.S., 1990. Revised world maps and introduction. In: Mckerrow, W.S., Scotese, C.R. (Eds.), Palaeozoic Palaeogeography and Biogeography. Geological Society, London, Memoir 12, pp. 1–21.
Sengor, A.M.C., 1990. A new model for the late Palaeozoic–Mesozoic tec-tonic evolution of Iran and its implications for Oman. In: Robertson, A.H.F., Searle, M.P., Ries, A.C. (Eds.), The Geology and Tectonics of the Oman Region, Geological Society of London, Special Publication 49, pp. 797–831.
Sengor, A.M.C., Altiner, D., Cin, A., Ustaomer, T., Hsu, K.J., 1988. Ori-gin and assembly of the Tethysides orogenic collage at the expense of Gondwana Land. In: Audley-Charles, M.G., Hallam, A. (Eds.), Gondwana and Tethys, Geological Society of London, Special Publication 37, pp. 119–181.
Sharland, P.R., Archer, R., Casey, D.M., Davies, R.B., Hall, S.H., Hevard, A.P., Horbury, A.D., Simmons, M.D., 2001. Arabian Plate Sequence Stratigraphy. GeoArabian, Special Publication 2, p. 270.
Shinn, E.A., 1983. Tidal flat environment. In: Scholle, P.A., Bebout, D.G., Moore, C.H. (Eds.), Carbonate Depositional Environments. American Association Petroleum Geologists Memoir, pp. 173–210.
Shinn, E.A., 1986. Modern Carbonate Tidal Flats: Their Diagnostic Features. Colorado School of Mines Quarterly 81, pp. 7–35.
Sloss, L.L., Speed, R.C., 1974. Relationships of cratonic and continental margin tectonic episodes. In: Dickinson, W.R. (Ed.), Tectonics and Sedimentation. The Society of Economic Paleontologists and Mineralogists Tulsa, Oklahoma, USA, Special Publication 22, pp. 98–119.
Spalletti, L.A., Poiré, D.G., Schwartz, E., Veiga, G.D., 2001. Sedimentologic and sequence stratigraphic model of a Neocomian marine carbonate-siliciclastic ramp: Neuquén Basin, Argentina. Journal of South America Earth Sciences 14, 609–624.
Stocklin, J., 1968. Structural history and tectonics of Iran: a review. American Association of Petroleum Geologists Bulletin 52, 1229–1258.
Stocklin, J., 1974. Possible ancient continental margins in Iran. In: Burk, C.A., Drake, C.L. (Eds.), The Geology of Continental Margins. Springer-Verlag, Berlin and Heidelberg, pp. 873–887.
Stocklin, J., 1977. Structural correlation of the Alpine ranges between Devonian–lower carboniferous of Iran and Central Asia. Memoires horsSerie de la Societe Geologique de France 8, 333–353.
Stocklin, J., Eftekhar-Nezhad, J., Hushmand-Zadeh, A., 1965. Geology of the Shotori Range (Tabas Area, East Iran). Geological Survey of Iran, Reports 3, p. 69 (in Persian).
Strand, K., 2005. Sequence stratigraphy of the silisiclastic East puolanka group, the palaeoproterozoic Kainuu Belt, Finland. Sedimentary Geology 176, 149–166.
Takin, M., 1972. Iranian geology and continental drift in the Middle East. Nature 235, 147–150.
Tomasovych, A., 2004. Microfacies and depositional environment of an upper triassic intra-platform carbonate basin: the fatric unit of West Carpathians (Slovakia). Facies 50, 77–105.
Torsvik, T.H., Cocks, L.R.M., 2009. The Lower Palaeozoic Palaeogeographical Evolution of the Northeastern and Eastern Peri-Gondwanan Margin from Turkey to New Zealand. Geological Society, London, Special Publications 325, pp. 3–21.
Torsvik, T.H., Cocks, L.R.M., 2013. Gondwana from top to base in space and time. Gondwana Research 24, 999–1030.
Tucker, M.E., Wright, V.P., 1990. Carbonate Sedimentology. Blackwells, Oxford, p. 482.
Tucker, M.E., 2001. Sedimentary Petrology: an Introduction to the Origin of Sedimentary Rocks. Blackwell, Scientific Publication, London, p. 262.
Tucker, M.E., Calvet, F., Hunt, D., 1993. Sequence stratigraphy of carbonate ramps: systems tracts, models and application to the Muschelkalk carbonate platform of eastern Spain. In: Posamentier, H.W., Summerhayes, C.P., Haq, B.U., Allen, G.P. (Eds.), Sequence Stratigraphy and Facies Associations, International Association of Sedimentology, Special Publication, vol. 18, pp. 397–415.
Vahdati-Daneshmand, F., Mosavvary, F., Mahmudy Ghareei, M.H., Ghasemi, A., 1995. Geological Map of Zarand, 1:100,000 Series. Sheet 7351, Geology Survey of Iran, Tehran.
Van Buchem, F.S.P., Razin, P., Homewood, P.W., Oterdoom, W.H., Philip, J., 2002. Straigraphic organization of carbonate ramps and organic rich intrashelf basins: Natih formation (middle Cretaceous) of northern Oman. American Association of Petroleum Geologists Bulletin 86, 21–53.
Vail, P.R., Mitchum Jr., R.M., Thompson, S., 1977. Seismic stratigraphy and global changes of sea level, part four: global cycles of relative changes of sea level. In: Payton, C.E. (Ed.), Seismic Stratigraphy Application to Hydrocarbon Exploration AAPG Memoir 26, pp. 83–98.
Walker, R.G., 2006. Facies models revisited: introduction. In: Posamentier, H.W., Walker, R.G. (Eds.), Facies Models Revisited SEPM Special Publication 84, pp. 1–17.
Warren, J.K., 2006. Evaporites: Sediments, Resources and Hydrocarbons. Springer-Verlag, Berlin and Heidelberg, p. 1035.
Webster, G.D., Maples, C.G., Mawson, R., Dastanpour, M., 2003. A cladid-dominated lower Mississipian crinoid and conodont fauna from Kerman Province, Iran, and revision of the glossocrinids and rhenocrinids. Journal of Paleontology 77, 35. Lawrence, Kansas.
Wehrmann, A., Yılmaz, I., Yalçın, M.N., Wilde, V., Schindler, E., Weddige, K., Demirtas, G.S., Özkan, R., Nazik, A., Nalcıoglu, G., Kozlu, H., Karslıoglu, O., Jansen, U., Ertug, K., 2010. Devonian shallow-water sequences from the North Gondwana coastal margin (Central and East-ern Taurides, Turkey): sedimentology, facies and global events. Gondwana Research 17, 546–560.
Wendt, J., Hayer, J., Karimi-Bavandpour, A., 1997. Stratigraphy and depositional environment of Devonian sediments in northeast and east-centralIran. Neues Jahrbuch fur Geologie und Palaontologie Abhandlungen 206, 277–322.
Wendt, J., Kaufmann, B., Belka, Z., Farsan, N., Karimu-Bavandpur, A., 2002. Devonian/lower Carboniferous stratigraphy, facies patterns and paleogeography of Iran, Part I. Southeastern Iran. Acta Geologica Polonica 52, 129–168.
Wendt, J., Kaufmann, B., Belka, Z., Farsan, N., Karimu-Bavandpur, A., 2005. Devonian/lower Carboniferous stratigraphy, facies patterns and paleogeography of Iran Part II. Northern and central Iran. Acta Geologica Polonica 55, 31–97.
Wilmsen, M., Fürsich, F.T., Seyed-Emami, K.M., Majidifard, R., Zamani-Pedram, M., 2010. Facies analysis of a large-scale jurassic shelf-lagoon: the Kamar-e-Mehdi formation of east-central Iran. Facies 56, 59–87.
Wilson, J.L., 1975. Carbonate Facies in Geologic History. Springer-Verlag, New York, p. 471.
Zand-Moghadam, H., Moussavi-Harami, R., Mahboubi, A., 2014. Sequence stratigraphy of the early–middle Devonian succession (Padeha Formation) in Tabas block, east-central Iran: implication for mixed tidalflat deposits. Palaeoworld 218, 1–19.